THE JOURNAL OF PHYSICAL CHEMISTRY A

Article

pubs.acs.org/JPCA

Theoretical Investigation of the Adsorption Properties of CO, NO, and OH on Monometallic and Bimetallic 13-Atom Clusters: The Example of Cu_{13}, Pt_7Cu_6, and Pt_{13}

Anderson S. Chaves,[†] Maurício J. Piotrowski,[‡] Diego Guedes-Sobrinho,[†] and Juarez L. F. Da Silva*[,†]

[†]São Carlos Institute of Chemistry, University of São Paulo, P.O. Box 780, 13560-970, São Carlos, SP, Brazil

[‡]Physics Department, Federal University of Pelotas, P.O. Box 354, 96010-900, Pelotas, RS, Brazil

Supporting Information

ABSTRACT: We report a density functional theory investigation of the adsorption properties of CO, NO, and OH on the Cu_{13}, Pt_7Cu_6, and Pt_{13} clusters in the cationic, neutral, and anionic states with the aim to improve our atomistic understanding of the adsorption properties on bimetallic clusters compared with monometallic clusters. The adsorption energy of CO and NO are substantially stronger on Pt_{13} than on Cu_{13}, and hence, CO and NO bind preferentially on Pt sites on Pt_7Cu_6. Thus, it can contribute to drive the migration of the Pt atoms from the core to the surface region in large PtCu nanoalloys. The CO and NO adsorption energies on the bimetallic cluster are enhanced by a few percent compared with the energies of the monometallic clusters, which shows that the Pt−Cu interaction can contribute to an increase in the adsorption energy. In contrast with CO and NO trends, the OH adsorption energies on Cu_{13}, Pt_7Cu_6, and Pt_{13} deviates only up to 0.31 eV, and hence, there is no clear preference for Cu or Pt sites on Pt_7Cu_6 or an enhancement of the adsorption energy on the bimetallic systems. We found a reduction of the CO and NO vibrational frequencies upon adsorption, which indicates a weakening of the CO and NO binding energies, and it is supported by a slight increase in the bond lengths. However, the OH vibrational frequency increases upon adsorption, which indicates an enhancement of the OH binding energy, which is supported by a slight decrease in the bond length by about 0.01 Å. It can be explained by the large charge transfer from the clusters to the O atom, which enhances the electrostatic interaction in the O−H bonding.

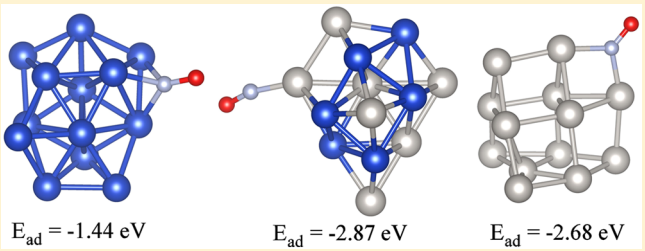

I. INTRODUCTION

Bimetallic transition-metal (TM) clusters with diameters less than 1 nm (e.g., about 45−55 TM atoms) have attracted great attention for several years,[1−3] in particular, because their physical and chemical properties change nonmonotonically with the number of atoms (i.e., every atom counts at this size regime),[1−6] atomic structure (e.g., low-symmetry configurations with a wide range of coordination sites),[3,7−10] charge states (cationic, neutral, anionic),[3,6,11,12] nature of the localization of the d-states,[5,8,13,14] and the chemical composition.[1−3,14−19] Although the dependence of the properties is complex, this behavior opens the possibility to tune the properties (e.g., center of gravity of the d-states) as a function of the physical parameters.[1−3] For example, recently, it was found by density functional theory (DFT) calculations[19] that the chemical composition in bimetallic PtTM nanoalloys (TM = Fe, Co, Ni, Cu, Zn) can be used to tune the position of the center of gravity of the occupied d-states, ϵ_d, of the surface atoms with respect to the highest occupied molecular orbital (HOMO) for 55-atom nanoalloys (i.e., ϵ_d can be shifted toward or away from the HOMO state), which can affect the adsorption energy of molecular species.[20,21]

Several experimental studies have indicated that monometallic and bimetallic TM clusters are promising for catalytic applications.[22,23] For example, monometallic Pt_8 clusters supported on aluminum oxide (Al_2O_3) are from 40 to 100 times more active for oxidative dehydrogenation of propane than macroscopic conventional catalysts,[22] which confirms that size effects can play a major role in chemical properties at this size. Bimetallic TM systems have been investigated as catalysts for several reactions,[4,24] such as preferential oxidation of CO in hydrogen by core−shell RuPt nanoalloys,[25,26] methane dehydrogenation by bimetallic AuPd clusters,[27] electrooxidation of formic acid by core−shell AuPt nanoalloys,[28] oxidation of benzyl alcohol by AuPd nanoalloys,[29] and oxygen reduction reactions using PtCu nanoalloys.[23,30]

Those studies have motivated a large number of theoretical studies with the aim to obtain an atomistic understanding of the physical and chemical properties of bimetallic TM clusters, in particular, for the PtCu systems[14,16,18,19] due to the large expectations raised by the recent experimental studies for PtCu

Received: August 26, 2015
Revised: October 27, 2015
Published: November 2, 2015

DOI: 10.1021/acs.jpca.5b08330
J. Phys. Chem. A 2015, 119, 11565−11573

nanoalloys.[23,30−36] For example, recently, Chaves et al.[18] reported a systematic investigation of bimetallic PtCu systems based on DFT calculations. They found a negative excess energy for all studied compositions from 3- to 14-atom clusters, which is in reasonable agreement with the excess energy obtained by previous DFT calculations for 12-atom PtCu clusters,[14] as well as with bimetallic 55-atom PtCu nanoclusters.[19] A structural analysis of the distribution of the Pt and Cu atoms shows a strong tendency of Cu by regions near the center of gravity of the clusters for both 13- and 55-atom model systems, which maximize the number of Pt atoms exposed to the vacuum region.[18,19] Furthermore, those findings clearly indicate that the formation of core−shell like structures starts at the small size regime.[18,19] Additionally, they found that the average bond length increases almost linearly by increasing the Pt composition, which can be explained by the larger atomic radius of the Pt atoms compared with the Cu atom radius.

Those theoretical studies[14,16,18,19] have addressed mainly the structural and electronic properties of the PtCu clusters; however, even using chemical descriptors such as chemical potential and global hardness[14,37,38] is not straightforward to stablish a connection between electronic (density of states, electron density) and reactivity properties, in particular for small bimetallic TM clusters. For example, the d-band model proposed by Nørskov works very well for surfaces;[20,21] however, it has difficulties for the adsorption of molecular species such as NO on small TM clusters,[39] which can be attributed to the discrete nature of the electronic d-states that affects the linear relation between coordination and the center of gravity of the occupied d-states. Thus, although several theoretical studies have been reported for small bimetallic PtCu clusters, our current understand is far from complete.

Therefore, to address this problem and to improve our atomistic understanding of the chemical properties of small bimetallic PtCu clusters, in particular 13-atom bimetallic PtCu models, we selected a set of molecules, namely, CO, NO, and OH, which play a crucial role in several chemical reactions.[20,21,31,40] Furthermore, they have been employed to probe the chemical reactivity of TM surfaces for decades,[38,41] and hence, the interaction mechanism of those molecular systems with TM surfaces have been discussed in details (e.g., donation back-donation model for CO and NO on TM surfaces),[39,41−49] which can helps to understand the interaction with bimetallic PtCu clusters. For comparison, we studied also the interaction of CO, NO, and OH with the Cu_{13} and Pt_{13} clusters for three different charge states, namely, cationic, neutral, and anionic.

II. THEORETICAL APPROACH AND COMPUTATIONAL DETAILS

A. Total Energy Calculations. Our calculations are based on spin-polarized DFT within the Perdew−Burke−Ernzerhof[50] (PBE) formulation for the exchange−correlation energy functional. To solve the Kohn−Sham (KS) equations, we expanded the KS molecular orbitals in numerical atom-centered orbitals (NAOs),[51,52] as implemented in the all-electron full-potential Fritz−Haber Institute *ab initio* molecular simulations (FHI-aims) package.[53,54] The electrons are treated using the scalar-relativistic framework within the atomic zeroth-order relativistic approximation[55] (*atomic* ZORA), where the binding energies differ slightly from *scaled* ZORA. For example, the binding energy per atom of Pt_{13} changes from −3.89 eV (*atomic* ZORA) to −3.91 eV (*scaled* ZORA), i.e., a difference of only 0.02 eV per atom.

We employed the NAO basis set called *tight-tier2* (using FHI-aims terminology) for Cu and Pt atoms and *tight-tier3* for C, O, N, and H atoms. The total energy convergence was set up to 1.0×10^{-5} eV, whereas a Gaussian broadening parameter of 10 meV was used for all calculations, except for the CO, NO, and OH molecules, where we employed 1 meV, which is important to obtain the correct spin multiplicity. For all total energy calculations, we employed initial electron densities based on the superposition of the free-atom electron densities, in which the free-atom electronic states were occupied on the basis of the Hund's rule for free atoms. Thus, all total energy calculations started with a high spin multiplicity, which was relaxed along the self-consistency field and geometric optimization. Thus, all the obtained spin multiplicities are a result of the calculation itself and not from constained calculations. The geometric optimizations were performed using the modified Broyden−Fletcher−Goldfarb−Shanno (BFGS) algorithm,[56] as implemented in FHI-aims. The equilibrium geometry was obtained once the atomic forces on every atom are smaller than 1.0×10^{-2} eV/Å.

B. Atomic Configurations. Although there are small differences among the results reported for Cu_{13},[6,7,57,58] Pt_7Cu_6,[18] and Pt_{13},[6,7,57,58] the main features are preserved, namely, those 13-atom systems in the putative global minimum configurations (GMC) adopt low coordinated structures instead of compact structures based on the icosahedral (ICO) or cuboctahedral (CUB) models.[59] Although there are a large number of high energy isomers beyond of the putative GMC, at experimental conditions, the GMC is one of the most probable structures to exist, even considering entropic effects. Thus, the putative GMC can be considered as one of the best candidates to study and understand the adsorption properties of molecular species on clusters. In this study, we employed the putative GMC obtained for the neutral clusters reported and discussed elsewhere[6,18] as initial configurations to obtain the cationic and anionic structures using geometric optimizations.[6] Furthermore, we mention that an adsorption study on all high energy isomers is not feasible due to the computational cost.

In contrast with low-Miller-index surfaces,[60] in which the number of high-symmetry adsorption sites are small and clearly defined, namely, 1-fold (top), 2-fold (bridge), 3-fold (hollow), and 4-fold sites,[47,48,61,62] the number of adsorption sites on the 13-atom clusters are larger as most of the atoms exposed to the vacuum region are nonequivalent because of the low symmetry of the clusters. For example, all the 1-fold sites, which includes all the TM atoms exposed to the vacuum region are nonequivalent, and hence, the adsorption would be different even if all the adsorption sites are 1-fold. Thus, there are several different 1-fold, 2-fold, 3-fold, and 4-fold sites, which were considered for the adsorption of CO, NO, and OH on the Cu_{13}, Pt_7Cu_6, and Pt_{13} clusters. For example, for CO/Pt_{13}, we considered 20 different adsorption sites and a similar number for the remaining systems. From the geometric optimization performed for every configuration, we obtained a hierarchical set of representative model structures (local minimum configurations) for each system, which will be discussed below.

III. RESULTS: DIATOMIC MOLECULES ADSORBED ON 13-ATOM CLUSTERS

The most important properties of CO, NO, OH, Cu_{13}, Pt_7Cu_6, and Pt_{13} in the gas phase are discussed in the Supporting

DOI: 10.1021/acs.jpca.5b08330
J. Phys. Chem. A 2015, 119, 11565−11573

Information. The putative lowest energy DFT-PBE structures for the Cu_{13}, Pt_7Cu_6, and Pt_{13} clusters in the neutral charge state are shown in the Figure 1. Following the procedure

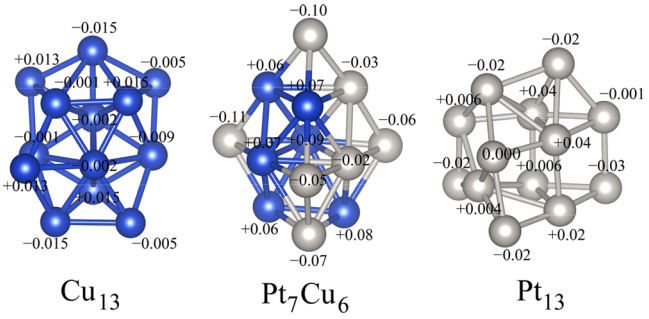

Figure 1. Lowest energy DFT-PBE structures for the Cu_{13}, Pt_7Cu_6, and Pt_{13} clusters in the neutral charge state. The numbers near each atom indicate the Hirshfeld charges, in number of *e*.

outlined in section II, we obtained the lowest energy configurations for CO, NO, and OH (MO) adsorbed on the Cu_{13}, Pt_7Cu_6, and Pt_{13} clusters in the cationic, neutral, and anionic states, Figure 2, and a large set of high energy isomers. Afterward, to obtain a deep understanding of the adsorption properties, we calculated the energetics, structural, electronic, and vibrational properties of the lowest energy, Table 1, and high-energy configurations (Supporting Information).

A. Adsorption Site Preference. In the lowest energy configurations, Figure 2, we found that CO binds preferentially on 1-fold TM sites with the C atom pointing toward the 13-atom clusters for all systems and charge states (e.g., 1-fold Cu sites on Cu_{13}, 1-fold Pt sites on Pt_{13} and also on Pt_7Cu_6). Thus, there is a preference of CO by Pt sites on Pt_7Cu_6. The 1-fold adsorption site preference is a common feature also on compact and stepped TM surfaces,[63] where the CO bond is perpendicular to the surface. The angle TMCO is nearly 180°. In contrast with CO, the adsorption sites of NO depend on the system and charge state. For example, NO binds with N pointing toward the clusters on the 1-fold Pt site on $(Pt_7Cu_6)^{+/0/-}$, 2-fold Pt sites on $Pt_{13}^{+/0/-}$, 2-fold Cu sites on $Cu_{13}^{\pm}$, and 3-fold Cu site on Cu_{13}^{0}. For 1-fold sites, the angle between the TMNO atoms deviates from 180°, which is similar to the results obtained for NO adsorption on compact TM(111).[47−49] Thus, it indicates that the nature of the interaction might not be too much different.

OH binds with the O atom pointing toward the 13-atom clusters (with H atom bent toward the cluster), on which the adsorption site is 2-fold in most cases, except the 1-fold Pt site on $(Pt_7Cu_6)^-$ and 3-fold $PtCu_2$ site on $(Pt_7Cu_6)^+$. For OH/$(Pt_7Cu_6)^0$, OH binds on both Cu and Pt atoms, and hence, it indicates no preference among the Cu or Pt sites at the cluster surface. Thus, for OH adsorption, we observe a decrease in cluster selectivity, which we attribute to the increased OH oxidation power related with its condition like a radical. It enhances the Coulomb electrostatic contribution (ionic character), which leads to a lack in the metal cluster selectivity. The enhanced ionic character was indeed previously suggested from theoretical calculations of the differences in the electric dipole moment when the OH radical is approaching a metal surface.[40]

B. Adsorption Energy. The adsorption energy, E_{ad}, measures the magnitude of the binding energy of the molecular species to the cluster, and it is given by the following equation,

$$E_{ad} = E_{tot}^{(MO/TM_{13})^{+/0/-}} - E_{tot}^{(TM_{13})^{+/0/-}} - E_{tot}^{MO} \quad (1)$$

where $E_{tot}^{(MO/TM_{13})^{+/0/-}}$ and $E_{tot}^{(TM_{13})^{+/0/-}}$ are the total energies of the MO/TM_{13} and TM_{13} systems in the cationic, neutral, and anionic charge states, respectively, and E_{tot}^{MO} is the total energy of MO (CO, NO, OH) in the neutral charge state. The E_{ad} results are shown in Table 1 for the lowest energy configurations, whereas the dependence with the adsorption site as well as the E_{ad} results for all high energy isomers are reported in the Supporting Information.

The adsorption energy is substantially larger for CO and NO on $(Pt_{13})^{+/0/-}$ than on $(Cu_{13})^{+/0/-}$. For example, the differences range from 80% to 120%, and hence, those results can explain the strong preference of CO and NO by Pt adsorption sites on

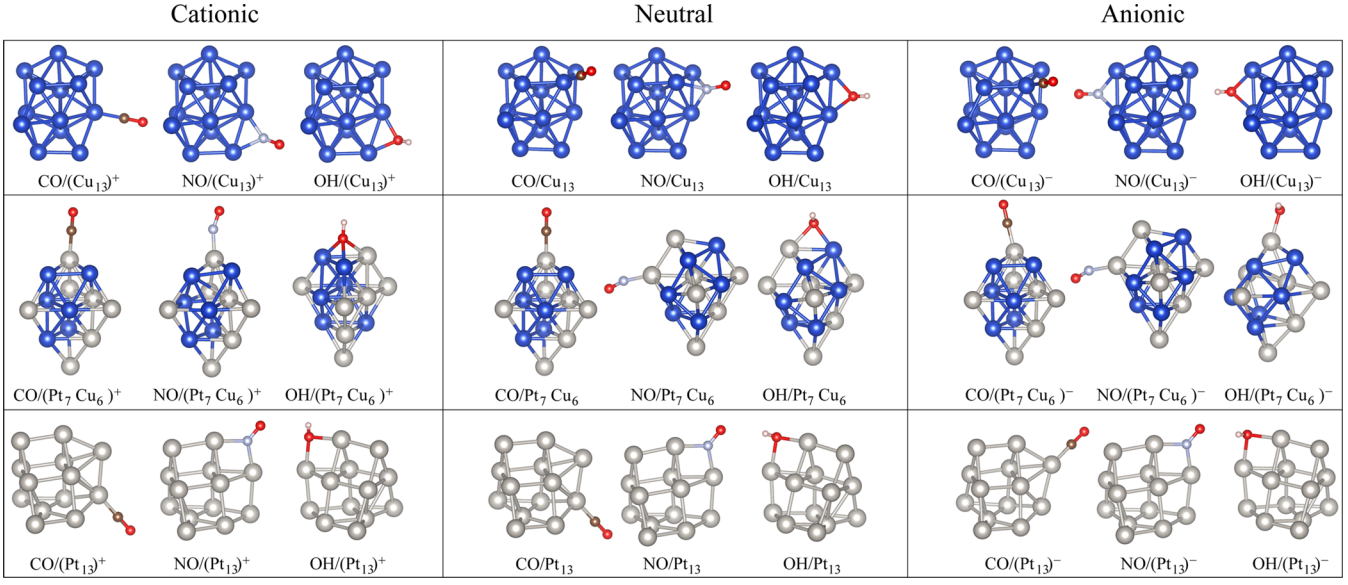

Figure 2. Lowest energy DFT-PBE configurations for the adsorption of CO, NO, and OH on the Cu_{13}, Pt_7Cu_6, and Pt_{13} clusters in the cationic, neutral, and anionic charge states.

DOI: 10.1021/acs.jpca.5b08330
J. Phys. Chem. A 2015, 119, 11565−11573

Table 1. Adsorption Properties of CO, NO, and OH on the Cu_{13}, Pt_7Cu_6, and Pt_{13} Clusters in the Cationic (+), Neutral (0), and Anionic (−) Charge States, in the Lowest Energy Configurations[a]

		Cu_{13}			Pt_7Cu_6			Pt_{13}		
		+	0	−	+	0	−	+	0	−
E_{ad} (eV)	CO	−1.37	−1.23	−1.33	−2.65	−2.65	−2.72	−2.48	−2.46	−2.41
	NO	−1.28	−1.44	−1.56	−2.92	−2.87	−2.90	−2.49	−2.68	−2.69
	OH	−3.42	−3.70	−3.55	−3.67	−3.69	−3.70	−3.73	−3.60	−3.49
d_{MO-TM} (Å)	CO	1.83	1.82	1.80	1.84	1.82	1.82	1.84	1.83	1.83
	NO	1.94	1.99	1.92	1.80	1.79	1.80	2.01	1.99	1.99
	OH	1.92	1.95	1.99	2.05	2.03	1.95	2.11	2.13	2.16
Δd_{av} (%)	CO	1.96	0.25	2.56	1.24	1.25	1.16	2.57	3.09	1.93
	NO	0.89	1.83	1.79	0.87	1.90	1.78	0.21	0.71	1.04
	OH	1.22	0.82	1.47	1.52	0.63	−0.81	−1.24	−0.85	−0.40
ΔECN (%)	CO	0.28	−0.28	−0.94	−0.77	1.10	1.56	12.59	15.28	−0.48
	NO	1.16	−2.13	−1.57	−12.17	0.36	−0.36	−17.13	−15.62	−15.64
	OH	0.95	−0.70	−0.09	−1.50	−9.76	−15.94	−20.90	−20.80	−20.99
d_0 (Å)	CO	1.14	1.15	1.16	1.15	1.16	1.17	1.15	1.16	1.17
	NO	1.20	1.22	1.22	1.16	1.17	1.19	1.19	1.21	1.22
	OH	0.97	0.97	0.97	0.97	0.97	0.97	0.98	0.97	0.97
ν (cm^{-1})	CO	2084	2031	1970	2042	1994	1941	2050	2008	1957
	NO	1573	1453	1519	1830	1767	1690	1583	1525	1469
	OH	3691	3708	3690	3670	3659	3664	3646	3654	3656
Q^{O}_{Hirs} (e)	CO	−0.03	−0.09	−0.14	−0.07	−0.12	−0.18	−0.07	−0.12	−0.16
	NO	−0.03	−0.12	−0.17	+0.02	−0.05	−0.12	−0.05	−0.12	−0.18
	OH	−0.31	−0.34	−0.36	−0.25	−0.28	−0.34	−0.24	−0.27	−0.29
Q^{C}_{Hirs} (e)	CO	+0.09	+0.05	+0.01	+0.08	+0.04	0.00	+0.08	+0.05	+0.02
Q^{N}_{Hirs} (e)	NO	−0.06	−0.09	−0.13	+0.05	0.00	−0.04	−0.01	−0.03	−0.06
Q^{H}_{Hirs} (e)	OH	+0.15	+0.12	+0.09	+0.18	+0.12	+0.09	+0.15	+0.12	+0.10

[a]Adsorption energy, E_{ad}; equilibrium MO−TM_{13} distance, d_{MO-TM}; relative changes in the average weighted cluster bond lengths, only for TM adsorption sites, due to the adsorption on TM_{13}, Δd_{av}; relative changes in the cluster effective coordination number (ECN), only for TM adsorption sites, due to the adsorption on TM_{13}, ΔECN; equilibrium bond length for CO, NO, and OH, d_0; vibrational frequencies of the adsorbed molecules, ν; and the Hirshfeld charges, Q_{Hirs}.

the bimetallic $(Pt_7Cu_6)^{+/0/-}$ clusters. Furthermore, the NO adsorption energy on Pt_{13} is about 51% larger than for NO/Pt(111) at 25% coverage,[47−49] which indicates an enhancement of the adsorption energy, in part due to the lower coordination of the adsorption sites on the 13-atom clusters. In contrast with CO and NO, we found a different trend for OH on the studied 13-atom clusters. For example, the adsorption energy is nearly the same for all systems and charge states (i.e., the largest differences are from 0.1 to 0.3 eV), and hence, we would expect no preference for Pt or Cu adsorption sites on $(Pt_7Cu_6)^{+/0/-}$, which is consistent with our findings for the adsorption site preference.

For CO and NO, which bind preferentially on Pt sites, we found an enhancement in the adsorption energy from 0.10 to 0.30 eV compared with the adsorption energy on Pt_{13} due to the formation of the Pt_7Cu_6 alloying (e.g., it changes from −2.46 eV for CO/Pt^0_{13} to −2.65 eV for $CO/(Pt_7Cu_6)^0$). Thus, the interaction of Pt with Cu atoms in the bimetallic Pt_7Cu_6 cluster contributes to enhances the adsorption energy, instead to decrease E_{ad} toward the values obtained for CO and NO on Cu_{13}. For OH, the trends are not clear as the adsorption energy increases or decreases by about 0.10−0.20 eV for OH on Pt_7Cu_6 compared with the case for the Cu_{13} and Pt_{13} clusters. The OH shows a strong interaction between O and TM atoms, which is larger than C or N interaction with TM atoms, Table 1. As previously reported,[64,65] this strong interaction occurs because TM atoms (adsorption sites) become oxidized (see Hirshfeld analysis below); consequently, there is no preference for adsorption sites and the adsorption energies are similar for all systems (i.e., the electrostatic interaction plays an important role).

C. Vibrational Frequencies. We found that vibrational frequencies of the CO and NO molecules decrease upon adsorption, which can be explained by the weakening of the CO and NO binding energies, in particular for NO on Cu_{13} (23%) and Pt_{13} (19%); however, it reduces only by about 6.4% for NO/Pt_7Cu_6. Thus, the alloy PtCu formation reduces the shift in the vibrational frequency. In contrast with CO and NO, we found an enhancement of the OH vibrational frequency upon adsorption from 1.6% to 3.1%, and hence, it indicates an enhancement of the OH binding energy. For CO and NO adsorption, the molecular vibrational frequencies decrease with the increase in the cluster charge state (cationic to anionic), indicating that the CO and NO molecular binding energies decrease with the cluster charge state. In turn, this feature is not true for OH adsorption, for example, the OH vibrational frequency is larger when adsorbed on $(Pt_{13})^-$ (3656 cm^{-1}) than on $(Pt_{13})^+$ (3646 cm^{-1}).

D. Geometric Parameters. The most important geometric parameters for the lowest energy configurations are summarized in Table 1, whereas the results for all the adsorption sites are shown in the Supporting Information. Compared with the gas-phase results, the equilibrium bond length of CO and NO, d_0, increases by 0.01 Å up to 0.06 Å upon adsorption on all systems and charge states, which indicates a slight weakening of the CO and NO binding energy. However, in contrast, we found a decreasing in the OH bond length by 0.01 Å, which indicates an enhancement in the strength of the OH binding

DOI: 10.1021/acs.jpca.5b08330
J. Phys. Chem. A 2015, 119, 11565−11573

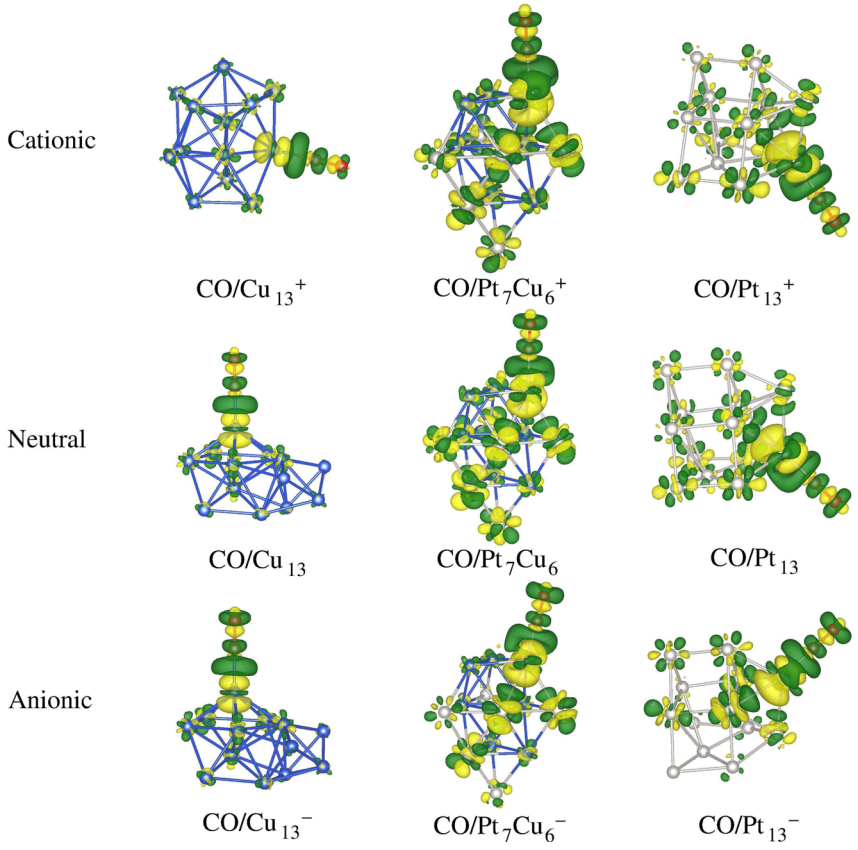

Figure 3. Difference electron density due to the CO adsorption on the 13-atom clusters (Cu_{13}, Pt_7Cu_6, Pt_{13}) for all lowest energy configurations in the cationic, neutral, and anionic charge states. The green regions in the isosurfaces indicate electron density accumulation, and yellow regions indicate electron density depletion, due to the adsorption.

energy, in agreement with vibration analysis. It can also be correlated with an enhancement of the charge transfer among the O and H atoms due to the interaction with the clusters. To characterize the distance of the molecules to the clusters, we calculated the smallest distance between the C (CO), N (NO), and O (OH) atoms to the nearest TM atoms, d_{MO-TM}. We found that d_{C-TM} = 1.80 Å up to 1.84 Å, which indicates a very small dependence on the chemical species and charge states, although there are large differences in the magnitude of the adsorption energies of CO on Cu_{13} and Pt_{13}. In constrast with CO, we found larger changes for NO. For example, d_{N-TM} = 1.79 Å ($(Pt_7Cu_6)^0$) up to 1.99 Å (Pt_{13}^0), which can be explained by the enhancement of the adsorption energy for NO/Pt_7Cu_6. For OH, we found that d_{O-TM} increases from Cu_{13} to Pt_7Cu_6 to Pt_{13} clusters; however, there is no correlation with the adsorption energy.

To address the structural changes in the clusters upon CO, NO, and OH adsorption, we selected only the adsorption sites, Table 1, and calculated the relative changes (in percentage) of the weighted bond length, d_{av}, and in the effective coordination number, ECN, with respect to the respective TM sites in the gas-phase clusters, namely, $\Delta d_{av} = (d_{av}^{MO/TM_{13}} - d_{av}^{TM_{13}}) \times 100/d_{av}^{TM_{13}}$ and $\Delta ECN = (ECN^{MO/TM_{13}} - ECN^{TM_{13}}) \times 100/ECN^{TM_{13}}$. The results for the deformation caused on all TM atoms (whole cluster) due to the adsorption process are shown in the Supporting Information and indicate that the major deformations indeed occur on the TM adsorption sites. We found that CO and NO induce an expansion of the TM−TM bond lengths in the adsorption sites for all systems from 0.21% to 3.09%; however, OH may induce expansions (Cu_{13}) or contractions (Pt_{13}) of the TM−TM bond lengths. The magnitude of the bond relaxations are similar to the interlayer relaxations in the topmost surface layers of compact TM(111) surfaces.[66−68] We found large values for ΔECN, in particular, for Pt_{13}, whereas the changes are very small for Cu_{13}. Our results indicate that the changes in the coordination of the adsorption site are not related with the magnitude of the adsorption energy.

E. Electron Density Difference. To illustrate the electron density redistribution on the molecules and clusters due to the interaction, we calculated the electron density difference, $\rho^{\Delta} = \rho^{MO/TM_{13}^{+,0,-}} - \rho^{TM_{13}^{+,0,-}} - \rho^{MO}$. The results for CO adsorption are shown in Figure 3, whereas the results for the remaining systems are shown in the Supporting Information. For all cases, we found a large electron density redistribution on the adsorption site in the cluster and on the diatomic molecules, which can be explained by the charge transfer among the chemical species with different electronegativities and polarization effects and the presence of the attractive cluster potential on the molecule states. The electron density redistribution on the Cu atoms are smaller than on the Pt atoms, which can be explained by the stronger interaction of CO with the Pt atoms and supported by large magnitude of the adsorption energy. Furthermore, the nature of d-states also contributes (e.g., the Cu 3d-states are completely filled and more localized than incomplete and more delocalized Pt 5d-states). The electron density redistributions are smaller near the TM atoms far from the adsorption site, which is expected as the redistribution is mainly related with the binding between

DOI: 10.1021/acs.jpca.5b08330
J. Phys. Chem. A 2015, 119, 11565−11573

molecules and clusters. From the electron density difference, we can identify that the d_{z^2}- (charge depletion) and $d_{x^2-y^2}$-orbitals play an important role in the interaction mechanism, which is expected as the d_{z^2}-orbital decreases its charge or/and polarizes easily compared with the remaining d-orbitals.[61,62,69] In contrast with the TM atoms, it is much harder to identify the orbitals that play a role in the electron density redistribution on the molecules.

F. Hirshfeld and Mulliken Charge Analysis. To obtain a quantitative description of the electron density redistribution, we calculate the Hirshfeld charges,[70,71] Q_{Hirs}, for all chemical species, Table 1 and Supporting Information. For comparison we also included the Mulliken population analysis[72,73] (Supporting Information) of each atom, where the effective Mulliken charge on every specie, Q_{eff}, can be calculated as $Q_{eff} = Z - Q_M$. Z is the atomic number, and Q_M is the Mulliken charge. The Mulliken charges have a strong dependence on the size of the basis set, whereas the electron density Hirshfeld analysis is quite robust with much smaller variations with the basis set size. Indeed, for systems with small charge transfer (e.g., $Q_{eff} < 0.1$ e), our Mulliken results show that the oscillations as a function of the basis set size is within the magnitude of the charge transfer of the systems; however, for systems with larger charge transfer both schemes show the same trends. Additionally, the Mulliken analysis yields the occupation of each atomic angular momentum channels in terms of the basis used (Supporting Information), which is not obtained by the Hirshfeld scheme as implemented in FHI-aims package.

From the Hirshfeld and Mulliken analyses, for the cationic and anionic systems, we found that about 70−100% of the electron was removed or located in the 13-atom clusters, respectively, which can be explained by the nature of the electronic states near to the HOMO and LUMO, i.e., mainly dominated by TM states. As shown in Figure 1, the Hirshfeld charges for the monometallic clusters are from −0.03 e to +0.04 e due to the presence of the vacuum region and different coordination environment for each atom, whereas in the bimetallic cluster, all the Cu atoms have a positive charge, namely, from 0.06 e to 0.09 e. Thus, the magnitude of the charge transfer from Cu to Pt atoms is nearly twice the charge transfer due to the environment and coordination effects. As CO adsorption energy is slightly weaker when Pt_{13} is negatively charged, it is counterintuitive to state that the charge transfer from Cu into Pt atoms in the bimetallic cluster leads into an increase in the adsorption energy, even though this argument is valid for NO adsorption. However, in addition to the charge transfer between Pt and Cu, the bimetallic cluster has a reduced number of Pt−Pt bonds in comparison with Pt_{13}, but an increased number of Pt−Cu bonds, whereas Pt atoms are undercoordinated in the bimetallic cluster. Hence, the CO and NO adsorption energies on Pt_7Cu_6 clusters are greater than on 13-atom Cu or Pt clusters, which can be explained by the charge transfer among the Pt−Cu species and the coordination of the adsorption sites.

Our Hirshfeld analysis indicates that, for the most cases the charge transfer follows the magnitude of the Pauling electronegativity, namely, χ = 3.44 (O), 3.04 (N), 2.55 (C), 2.28 (Pt), 2.2 (H), and 1.9 (Cu), on which is observed a net charge transfer from the Cu_{13}, Pt_7Cu_6, and Pt_{13} clusters into the CO, NO, and OH molecules. However, it is not the case for several systems, in particular, CO adsorbed on cationic systems and NO adsorbed on the cationic Pt_7Cu_6 cluster. Only for such cases did we notice that the O atom decreases its charge. In turn, the O atom tends to increase its charge for the remaining systems, and hence, the CO and OH dipole moments are expected to increase compared with the gas-phase values. In contrast with CO and OH, we found that NO shows a different behavior on Cu_{13} and Pt_{13}. For example, in the gas phase, the effective charge on the N and O atoms are very small (e.g., 0.01 e), which implies a small dipole moment, which changes upon adsorption. Our results show that Cu atoms donate charge to the N atom (i.e., changes from +0.01 e to −0.13 e), while the charge on O atom increases. Thus, it contributes to increase the Coulomb repulsion between the N and O atoms, and hence, it helps to explain the substantial increase in the NO bond length upon adsorption on Cu_{13}.

Based on the Mulliken charge analysis discriminated for each atomic angular momentum channel (Supporting Information), our results show an electron donation from C and N into the cluster and a possible electron back-donation that affects the O atom, which is consistent with the well-known donation/back-donation mechanism used to explain the interaction of CO and NO with TM surfaces.[42,44] For all systems with an increase in the charge state (anionic systems) there is a clear tendency of TM clusters losing (back-donate) more charge or, at least, TM clusters gaining less charge from molecules. This feature is related with the Stark effect, i.e., a purely electrostatic change in the MO dipole−TM cluster electric field interactions, the same result obtained for CO adsorbed on neutral and charged Au clusters.[74]

G. Projected Density of States. To understand the changes in the electronic states upon adsorption, we calculated the projected density of states (PDOS) for every system (Supporting Information). As expected, we found that the HOMO and LUMO of the CO, NO, and OH are strongly affected upon adsorption; namely, there is a broadening of the HOMO and LUMO states, which plays a crucial role in the interaction mechanism. For example, the CO, NO, and OH HOMO states broaden and extend above the HOMO of the combined system, and hence, there is a depopulation of the HOMO, while a tail of the LUMO extends to the occupied region. For CO and NO interactions, the LUMO composed of the antibonding $2\pi^*$ states (Supporting Information) becomes more populated (shift down) with the increase of the cluster charge states (anionic systems), enhancing the back-donation process, and hence, decreasing the CO and NO binding energy, increasing their bond lengths, and decreasing their vibrational frequencies, as discussed above. For OH adsorption, the main interaction occurs through the nonbonding HOMO/LUMO 1π valence orbital, and hence, the partial filling of the nonbonding 1π state does not cause such noticeable changes in the OH molecular bonds; that is, the OH bond lengths tend to be the same when adsorbed on different systems (Table 1 and Supporting Information). Thus, these trends support our Hirshfeld and Mulliken analysis, which indicates a charge transfer among the chemical species. The broadening of the HOMO and LUMO contributes to enhance the hybridization with the TM states, which plays an important role in the magnitude of the binding energy.

IV. SUMMARY

We reported a DFT-PBE investigation of the adsorption properties of CO, NO, and OH on the Cu_{13}, Pt_7Cu_6, and Pt_{13} clusters in different charge states (cationic, neutral, and anionic) with the aim to obtain a better understanding of the

DOI: 10.1021/acs.jpca.5b08330
J. Phys. Chem. A 2015, 119, 11565−11573

adsorption properties on bimetallic clusters compared with the respective monometallic clusters. Our results for the gas-phase molecules and 13-atom clusters are consistent with experimental and previous theoretical calculations. We found that CO and NO bind preferentially on the Pt adsorption sites on Pt_7Cu_6, which can be explained by the substantial difference in the adsorption energy of CO and NO on the Cu_{13} and Pt_{13} clusters, i.e., binds stronger on the Pt_{13} cluster than on Cu_{13}. In principle, we would expect an adsorption energy between the limits for Pt_{13} and Cu_{13}; however, we found an enhancement of the adsorption energy on the bimetallic cluster compared with the energy for Pt_{13}, which indicates that the interaction of Pt−Cu can contribute to an increase in the adsorption energy, related with the charge transfer among both species obtained from our Hirshfeld analysis as well as the consequent reduction of the coordination of Pt atoms with an enhanced number of Pt−Cu bondings in the bimetallic cluster. We found a reduction of the CO and NO vibrational frequencies upon adsorption, in particular for NO, which indicates a weakening of the CO and NO binding energies.

The OH adsorption properties follow a different trend compared with those for CO and NO. The adsorption energy values are almost the same on Cu_{13}, Pt_7Cu_6, and Pt_{13} and for different charge states, i.e., deviations from 0.00 to 0.31 eV are observed among all systems. The OH adsorption energy is larger than CO and NO values because of a strong interaction between O and TM atoms. The TM atoms involved in the adsorption sites become oxidized (as shown by their positive atomic Hirshfeld charges), and hence, we would expect no preference for Pt or Cu adsorption sites on $(Pt_7Cu_6)^{+/0/-}$, which is consistent with our findings. The OH vibrational frequency increases upon adsorption, which indicates an enhancement of the OH binding energy and correlates well with a slight decrease in the bond length by about 0.01 Å. This trend can be explained by the large charge transfer from the clusters to the O atom, which enhances the electrostatic interaction between the O and H atoms, as well as between the oxidized TM atoms (positive) and the negatively charged O atom.

■ ASSOCIATED CONTENT

Supporting Information

The Supporting Information is available free of charge on the ACS Publications website at DOI: 10.1021/acs.jpca.5b08330.

Discussion of the gas-phase system including tables of diatomic molecular and transition-metal cluster properties, adsorption energies, Hirshfeld population analysis, Mulliken analysis, and tests for different charge population analysis schemes and figures of molecular orbital energies and their decomposition, adsorption energies, equilibrium bond lengths, relative deviations in the average weighted bond lengths and in the effective coordination number, charge density difference structures, and projected DOS. (PDF)

■ AUTHOR INFORMATION

Corresponding Author

*E-mail: juarez_dasilva@iqsc.usp.br. Phone: +55 16 3373 6641. Fax: +55 16 3373 9952.

Notes

The authors declare no competing financial interest.

■ ACKNOWLEDGMENTS

We thank the National Council of Technological and Scientific Development, CNPq, the Coordination for the Improvement of Higher Level Education, CAPES, the São Paulo Research Foundation, FAPESP, and the Rio Grande do Sul Research Foundation, FAPERGS. We also thank the infrastructure provided to our computer cluster by the São Carlos Center of Informatics, University of São Paulo.

■ REFERENCES

(1) Ferrando, R.; Jellinek, J.; Johnston, R. L. Nanoalloys: From Theory to Applications of Alloy Clusters and Nanoparticles. *Chem. Rev.* **2008**, *108*, 845−910.

(2) Jellinek, J. Nanoalloys: Tuning Properties and Characteristics Through Size and Composition. *Faraday Discuss.* **2008**, *138*, 11−35.

(3) Ferrando, R. Symmetry Breaking and Morphological Instabilities in Core-Shell Metallic Nanoparticles. *J. Phys.: Condens. Matter* **2015**, *27*, 013003.

(4) Baletto, F.; Ferrando, R. Structural Properties of Nanoclusters: Energetic, Thermodynamic, and Kinetic Effects. *Rev. Mod. Phys.* **2005**, *77*, 371−423.

(5) Da Silva, J. L. F.; Piotrowski, M. J.; Aguilera-Granja, F. Hybrid Density Functional Study of Small Rh_n (n = 2−15) Clusters. *Phys. Rev. B: Condens. Matter Mater. Phys.* **2012**, *86*, 125430.

(6) Chaves, A. S.; Rondina, G. G.; Piotrowski, M. J.; Tereshchuk, P.; Da Silva, J. L. F. The Role of Charge States in the Atomic Structure of Cu_n and Pt_n (n = 2−14 Atoms) Clusters: A DFT Investigation. *J. Phys. Chem. A* **2014**, *118*, 10813−10821.

(7) Piotrowski, M. J.; Piquini, P.; Da Silva, J. L. F. Density Functional Theory Investigation of 3*d*, 4*d*, and 5*d*13-atom Metal Clusters. *Phys. Rev. B: Condens. Matter Mater. Phys.* **2010**, *81*, 155446.

(8) Piotrowski, M. J.; Piquini, P.; Cândido, L.; Da Silva, J. L. F. The Role of Electron Localization in the Atomic Structure of Transition-Metal 13-Atom Clusters: The Example of Co_{13}, Rh_{13}, and Hf_{13}. *Phys. Chem. Chem. Phys.* **2011**, *13*, 17242−17248.

(9) Lu, Y.; Chen, W. Sub-nanometre Sized Metal Clusters: From Synthetic Challenges to the Unique Property Discoveries. *Chem. Soc. Rev.* **2012**, *41*, 3594−3623.

(10) Rondina, G. G.; Da Silva, J. L. F. A Revised Basin-Hopping Monte Carlo Algorithm for Structure Optimization of Clusters and Nanoparticles. *J. Chem. Inf. Model.* **2013**, *53*, 2282−2298.

(11) Furche, F.; Ahlrichs, R.; Weis, P.; Jacob, C.; Gilb, S. The Structures of Small gold Cluster Anions as Determined by a Combination of Ion Mobility Measurements and Density Functional Calculations. *J. Chem. Phys.* **2002**, *117*, 6982−6990.

(12) Yoon, B.; Häkkinen, H.; Landman, U.; Wörz, A. S.; Antonietti, J.-M.; Abbet, S.; Judai, K.; Heiz, U. Charging Effects on Bonding and Catalyzed Oxidation of CO on Au_8 Clusters on MgO. *Science* **2005**, *307*, 403.

(13) Alonso, J. A. Electronic and Atomic Structure, and Magnetism of Transition-Metal Clusters. *Chem. Rev.* **2000**, *100*, 637−678.

(14) Mejía-López, J.; García, G.; Romero, A. H. Physical and Chemical Characterization of $Pt_{12-n}Cu_n$ Clusters via Ab-initio Calculations. *J. Chem. Phys.* **2009**, *131*, 044701.

(15) Aguado, A.; López, J. M. Identifying Structural and Energetic Trends in Isovalent Core-Shell Nanoalloys as a Function of Composition and Size Mismatch. *J. Chem. Phys.* **2011**, *135*, 134305.

(16) Piotrowski, M. J.; Piquini, P.; Da Silva, J. L. F. Platinum-Based Nanoalloys Pt_nTM_{55-n} (TM = Co, Rh, Au): A Density Functional Theory Investigation. *J. Phys. Chem. C* **2012**, *116*, 18432−18439.

(17) Yu, W.; Porosoff, M. D.; Chen, J. G. Review of Pt-Based Bimetallic Catalysis: From Model Surfaces to Supported Catalysts. *Chem. Rev.* **2012**, *112*, 5780−5817.

(18) Chaves, A. S.; Rondina, G. G.; Piotrowski, M. J.; Da Silva, J. L. F. Structural Formation of Binary PtCu Clusters: A Density Functional Theory Investigation. *Comput. Mater. Sci.* **2015**, *98*, 278−286.

(19) Guedes-Sobrinho, D.; Nomiyama, R. K.; Chaves, A. S.; Piotrowski, M. J.; Da Silva, J. L. F. Structure, Electronic, and Magnetic

DOI: 10.1021/acs.jpca.5b08330
J. Phys. Chem. A 2015, 119, 11565−11573

Properties of Binary Pt_nTM_{55-n} (TM = Fe, Co, Ni, Cu, Zn) Nanoclusters: A Density Functional Theory Investigation. *J. Phys. Chem. C* **2015**, *119*, 15669−15679.
(20) Hammer, B.; Nørskov, J. K. Electronic Factors Determining the Reactivity of Metal Surfaces. *Surf. Sci.* **1995**, *343*, 211−220.
(21) Nørskov, J. K.; Abild-Pedersen, F.; Studt, F.; Bligaard, T. Density Functional Theory in Surface Chemistry and Catalysis. *Proc. Natl. Acad. Sci. U. S. A.* **2011**, *108*, 937−943.
(22) Vajda, S.; Pellin, M. J.; Greeley, J. P.; Marshall, C. L.; Curtiss, L. A.; Ballentine, G. A.; Elam, J. W.; Catillon-Mucherie, S.; Redfern, P. C.; Mehmood, F.; Zapol, P. Subnanometre Platinum Clusters as Highly Active and Selective Catalysts for the Oxidative Dehydrogenation of Propane. *Nat. Mater.* **2009**, *8*, 213−216.
(23) Oezaslan, M.; Heggen, M.; Strasser, P. Size-Dependent Morphology of Dealloyed Bimetallic Catalysts: Linking the Nano to the Macro Scale. *J. Am. Chem. Soc.* **2012**, *134*, 514−524.
(24) Greeley, J.; Mavrikakis, M. Alloy Catalysts Designed from First Principles. *Nat. Mater.* **2004**, *3*, 810−815.
(25) Alayoglu, S.; Nilekar, A. U.; Mavrikakis, M.; Eichhorn, B. Ru-Pt Core-Shell Nanoparticles for Preferential Oxidation of Carbon Monoxide in Hydrogen. *Nat. Mater.* **2008**, *7*, 333−338.
(26) Alayoglu, S.; Zavalij, P.; Eichhorn, B.; Wang, Q.; Frenkel, A. I.; Chupas, P. Structural and Architectural Evaluation of Bimetallic Nanoparticles: A Case Study of Pt−Ru Core-Shell and Alloy Nanoparticles. *ACS Nano* **2009**, *3*, 3127−3137.
(27) Lang, S. M.; Frank, A.; Bernhardt, T. M. Composition and Size Dependent Methane Dehydrogenation on Binary Gold-Palladium Clusters. *Int. J. Mass Spectrom.* **2013**, *354*−*355*, 365−371.
(28) Fang, P.-P.; Duan, S.; Lin, X.-D.; Anema, J. R.; Li, J.-F.; Buriez, O.; Ding, Y.; Fan, F.-R.; Wu, D.-Y.; Ren, B.; Wang, Z. L.; Amatore, C.; Tian, Z.-Q. Tailoring Au-core Pd-shell Pt-cluster Nanoparticles for Enhanced Electrocatalytic Activity. *Chem. Sci.* **2011**, *2*, 531.
(29) Feng, J.; Ma, C.; Miedziak, P. J.; Edwards, J. K.; Brett, G. L.; Li, D.; Du, Y.; Morgan, D. J.; Hutchings, G. J. Au-Pd Nanoalloys Supported on Mg−Al Mixed Metal Oxides as a Multifunctional Catalyst for Solvent-Free Oxidation of Benzyl Alcohol. *Dalton Trans.* **2013**, *42*, 14498−14508.
(30) Strasser, P.; Koh, S.; Anniyev, T.; Greeley, J.; More, K.; Yu, C.; Liu, Z.; Kaya, S.; Nordlund, D.; Ogasawara, H.; Toney, M. F.; Nilsson, A. Lattice-Strain Control of the Activity in Dealloyed Core-Shell Fuel Cell Catalysts. *Nat. Chem.* **2010**, *2*, 454.
(31) Abdelsayed, V.; Aljarash, A.; El-Shall, M. S.; Al Othman, Z. A.; Alghamdi, A. H. Microwave Synthesis of Bimetallic Nanoalloys and CO Oxidation on Ceria-Supported Nanoalloys. *Chem. Mater.* **2009**, *21*, 2825−2834.
(32) Yang, H.; Dai, L.; Xu, D.; Fang, J.; Zou, S. Electrooxidation of Methanol and Formic Acid on PtCu Nanoparticles. *Electrochim. Acta* **2010**, *55*, 8000−8004.
(33) Oezaslan, M.; Hasché, F.; Strasser, P. In Situ Observation of Bimetallic Alloy Nanoparticle Formation and Growth Using High-Temperature XRD. *Chem. Mater.* **2011**, *23*, 2159−2165.
(34) Wang, D.; Yu, Y.; Xin, H. L.; Hovden, R.; Ercius, P.; Mundy, J. A.; Chen, H.; Richard, J. H.; Muller, D. A.; DiSalvo, F. J.; Abruña, H. D. Tuning Oxygen Reduction Reaction Activity via Controllable Dealloying: A Model Study of Ordered Cu_3Pt/C Intermetallic Nanocatalysts. *Nano Lett.* **2012**, *12*, 5230−5238.
(35) Yu, Z.; Zhang, J.; Liu, Z.; Ziegelbauer, J. M.; Xin, H.; Dutta, I.; Muller, D. A.; Wagner, F. T. Comparison between Dealloyed $PtCo_3$ and $PtCu_3$ Cathode Catalysts for Proton Exchange Membrane Fuel Cells. *J. Phys. Chem. C* **2012**, *116*, 19877−19885.
(36) Liu, L.; Samjeské, G.; Takao, S.; Nagasawa, K.; Iwasawa, Y. Fabrication of PtCu and PtNiCu Multi-Nanorods with Enhanced Catalytic Oxygen Reduction Activities. *J. Power Sources* **2014**, *253*, 1−8.
(37) Parr, R. G.; Pearson, R. G. Absolute Hardness: Companion Parameter to Absolute Electronegativity. *J. Am. Chem. Soc.* **1983**, *105*, 7512−7516.
(38) Scheffler, M.; Stampfl, C. *Theory of adsorption on metal substrates*; Hamdbook of Surface Science; Elsevier: Amsterdam, 2000; Vol. 2, pp 285−356.
(39) Piotrowski, M. J.; Piquini, P.; Zeng, Z.; Da Silva, J. L. F. Adsorption of NO on the Rh_{13}, Pd_{13}, Ir_{13}, and Pt_{13} Clusters: A Density Functional Theory Investigation. *J. Phys. Chem. C* **2012**, *116*, 20540.
(40) Koper, M. T.; van Santen, R. A. Interaction of H, O and OH with Metal Surfaces. *J. Electroanal. Chem.* **1999**, *472*, 126−136.
(41) Eyrich, M.; Diemant, T.; Hartmann, H.; Bansmann, J.; Behm, R. J. Interaction of CO with Structurally Well-Defined Monolayer PtAu/Pt(111) Surface Alloys. *J. Phys. Chem. C* **2012**, *116*, 11154−11165.
(42) Blyholder, G. Molecular Orbital View of Chemisorbed Carbon Monoxide. *J. Phys. Chem.* **1964**, *68*, 2772−2777.
(43) Hammer, B.; Morikawa, Y.; Nørskov, J. K. CO Chemisorption at Metal Surfaces and Overlayers. *Phys. Rev. Lett.* **1996**, *76*, 2141−2144.
(44) Glassey, W. V.; Hoffmann, R. A Comparative Study of the $p(2 \times 2)$-CO/M(111), M = Pt, Cu, Al Chemisorption Systems. *J. Phys. Chem. B* **2001**, *105*, 3245−3260.
(45) Ackermann, M. D.; Pedersen, T. M.; Hendriksen, B. L. M.; Robach, O.; Bobaru, S. C.; Popa, I.; Quiros, C.; Kim, H.; Hammer, B.; Ferrer, S.; Frenken, J. W. M. Strcture and Reactivity of Surface Oxides on Pt(110) During Catalytic CO Oxidation. *Phys. Rev. Lett.* **2005**, *95*, 255505.
(46) Falsig, H.; Hvolbæk, B.; Kristensen, I. S.; Jiang, T.; Bligaard, T.; Christensen, C. H.; Nøskov, J. K. Trends in the Catalytic CO Oxidation Activity of Nanoparticles. *Angew. Chem., Int. Ed.* **2008**, *47*, 4835−4839.
(47) Zeng, Z.-H.; Da Silva, J. L. F.; Deng, H.-Q.; Li, W.-X. Density Functional Theory Study of the Energetics, Electronic Structure, and Core-Level Shifts of NO Adsorption on the Pt(111) Surface. *Phys. Rev. B: Condens. Matter Mater. Phys.* **2009**, *79*, 205413.
(48) Zeng, Z.; Da Silva, J. L. F.; Li, W.-X. Theory of Nitride Oxide Adsorption on Transition Metal (111) Surfaces: A First-Principles Investigation. *Phys. Chem. Chem. Phys.* **2010**, *12*, 2459−2470.
(49) Zeng, Z.; Da Silva, J. L. F.; Li, W.-X. Desinty Functional Theory and Ab-initio Molecular Dynamics Study of NO Adsorption on Pd(111) and Pt(111) Surfaces. *Phys. Rev. B: Condens. Matter Mater. Phys.* **2010**, *81*, 085408.
(50) Perdew, J. P.; Burke, K.; Ernzerhof, M. Generalized Gradient Approximation Made Simple. *Phys. Rev. Lett.* **1996**, *77*, 3865−3868.
(51) Averill, F. W.; Ellis, D. E. An Efficient Numerical Multicenter Basis Set for Molecular Orbital Calculations: Application to $FeCl_4$. *J. Chem. Phys.* **1973**, *59*, 6412−6418.
(52) Zunger, A.; Freeman, A. J. Self-Consistent Numerical-Basis-Set Linear-Combination-of-Atomic-Orbitals Model for the Study of Solids in the Local Density Formalism. *Phys. Rev. B* **1977**, *15*, 4716−4737.
(53) Blum, V.; Gehrke, R.; Hanke, F.; Havu, P.; Havu, V.; Ren, X.; Reuter, K.; Scheffler, M. Ab Initio Molecular Simulations with Numeric Atom-Centered Orbitals. *Comput. Phys. Commun.* **2009**, *180*, 2175−2196.
(54) Havu, V.; Blum, V.; Havu, P.; Scheffler, M. Efficient O(N) integration for All-Electron Electronic Structure Calculation Using Numeric Basis Functions. *J. Comput. Phys.* **2009**, *228*, 8367−8379.
(55) van Lenthe, E.; Snijders, J. G.; Baerends, E. J. The Zero-Order Regular Approximation for Relativistic Effects: The Effect of Spin-Orbit Coupling in Closed Shell Molecules. *J. Chem. Phys.* **1996**, *105*, 6505−6516.
(56) Nocedal, J.; Stephen, J.; Wright, S. J. *Numerical Optimization*; Springer: Berlin, 2006.
(57) Sun, Y.; Zhang, M.; Fournier, R. Periodic Trends in the Geometric Structures of 13-Atom Metal Clusters. *Phys. Rev. B: Condens. Matter Mater. Phys.* **2008**, *77*, 075435.
(58) Chou, J. P.; Hsing, C. R.; Wei, C. M.; Cheng, C.; Chang, C. M. Ab Initio Random Structure Search for 13-Atom Clusters of FCC Elements. *J. Phys.: Condens. Matter* **2013**, *25*, 125305.
(59) Mackay, A. L. A Dense Non-Crystallographic Packing of Equal Spheres. *Acta Crystallogr.* **1962**, *15*, 916−918.

DOI: 10.1021/acs.jpca.5b08330
J. Phys. Chem. A 2015, 119, 11565−11573

(60) Desjonquères, M.-C.; Spanjaard, D. *Concepts in Surface Science*; Springer: Berlin, 1995.
(61) Da Silva, J. L. F.; Stampfl, C.; Scheffler, M. Adsorption of Xe Atoms on Metal Surfaces: New Insights from First-Principles Calculations. *Phys. Rev. Lett.* **2003**, *90*, 066104.
(62) Da Silva, J. L. F.; Stampfl, C.; Scheffler, M. Xe Adsorption on Metal Surfaces: First-Principles Investigations. *Phys. Rev. B: Condens. Matter Mater. Phys.* **2005**, *72*, 075424.
(63) Tereshchuk, P.; Freire, R. L. H.; Da Silva, J. L. F. The role of the CO Adsorption on Pt Monolayers Supported on Flat and Stepped Au Surfaces: A Density Functional Investigation. *RSC Adv.* **2014**, *4*, 9247−9254.
(64) Balbuena, P. B.; Altomare, D.; Vadlamani, N.; Bingi, S.; Agapito, L. A.; Seminario, J. M. Adsorption of O, OH, and H_2O on Pt-Based Bimetallic Clusters Alloyed with Co, Cr, and Ni. *J. Phys. Chem. A* **2004**, *108*, 6378−6384.
(65) Chibisov, A. N. Oxygen Adsorption on Small Ti Clusters: A First-Principles Study. *Comput. Mater. Sci.* **2014**, *82*, 131−133.
(66) Da Silva, J. L. F.; Schroeder, K.; Blügel, S. First-Principles Investigations of the Multilayer Relaxation of Stepped Cu Surfaces. *Phys. Rev. B: Condens. Matter Mater. Phys.* **2004**, *69*, 245411.
(67) Da Silva, J. L. F. All-Electron First-Principles Calculations of Clean Surface Properties of Low-Miller-Index Al Surfaces. *Phys. Rev. B: Condens. Matter Mater. Phys.* **2005**, *71*, 195416.
(68) Da Silva, J. L. F.; Stampfl, C.; Scheffler, M. Converged Properties of Clean Metal Surfaces by All-Electron First-Principles Calculations. *Surf. Sci.* **2006**, *600*, 703−715.
(69) Da Silva, J. L. F.; Stampfl, C. Trends in Adsorption of Noble Gases He, Ne, Ar, Kr, and Xe on Pd(111)($\sqrt{3} \times \sqrt{3}$) *R*30°: All-Electron Density-Functional Calculations. *Phys. Rev. B: Condens. Matter Mater. Phys.* **2008**, *77*, 045401.
(70) Hirshfeld, F. L. Bonded-atom Fragments for Describing Molecular Charge Densities. *Theor. Chim. Acta* **1977**, *44*, 129−138.
(71) Nalewajski, R. F.; Parr, R. G. Information Theory, Atoms in Molecules, and Molecular Similarity. *Proc. Natl. Acad. Sci. U. S. A.* **2000**, *97*, 8879−8882.
(72) Mulliken, R. S. Electronic Population Analysis on LCAO−MO Molecular Wave Functions. I. *J. Chem. Phys.* **1955**, *23*, 1833−1840.
(73) Jensen, F. *Introduction to Computational Chemistry*; Wiley: Chichester, U.K., 1999.
(74) Bagus, P. S.; Pacchioni, G. On the Origin of Bonding and Vibrational Frequency Shifts for CO Adsorbed on Neutral Cationic and Anionic Gold Clusters. *J. Phys. Conf. Ser.* **2008**, *117*, 012003.

DOI: 10.1021/acs.jpca.5b08330
J. Phys. Chem. A 2015, 119, 11565−11573